HYDRODYNAMIC DRAG OF THE DOLPHIN

T. E. Alekseeva and B. N. Semenov

An experimental study of the hydrodynamic drag of the dolphin is reported. The results are compared with calculations for the steady-state motion of a similar rigid model, and previously reported data on the hydrodynamic drag of the dolphin are refined. The drag turns out to be much less than the calculated drag, even when the initial laminar region is taken into account. Several conclusions can be drawn from the results: 1) The experimental results show quite reliably that hydrodynamically the dolphin is in fact a unique phenomenon. 2) The phenomenon is explained in terms of Gray's paradox for the dolphin. 3) The mechanism by which the dolphin's drag is reduced is apparently controllable. 4) Flow around the dolphin can be assumed to be laminar undetached flow.

1. Experimental Procedure

The procedure used previously by one of the authors [1] was refined so that the error in the drag measurement was reduced by a factor of about two. Previously, a study was made of the temporal and spatial motion of the dolphin, and then the velocity and acceleration were found through differentiation with respect to time; the second differentiation involves extremely large errors. In the refined experimental procedure, the dolphin velocity was determined by a comparison with the velocity of a standard sphere 6 mm in diameter falling in a tube having an i.d. of 12 mm and photographed by a motion-picture camera along with the dolphin motion.

The acceleration was calculated as the first time derivative of the measured velocity. The experiments were carried out with Tursiops (tursio) ponticus dolphins. The dolphin drag was determined during inertial motion from

$$R = (m + \lambda_{11})\, a$$

where a is the deceleration, m is the mass of the dolphin (determined by weighing), and λ_{11} is the attached mass of water for motion along the axis of the object, determined by calculation [1].

The dolphin and spheres were photographed under water by three Konvasavtomat motion-picture cameras in metal boxes. The optical axes of the cameras were held parallel. We used DS-5 film and RO-70 objective lenses having a focal length of F = 22 mm. A white screen was used for improved contrast.

The apparatus was arranged as described in [1]; the cameras were turned on simultaneously and operated by remote control. The film was processed in the following manner:

1) Sequences were selected for processing; a necessary condition was that there be no lateral motion of the tail.

2) The yaw angle of the dolphin was determined, and its constancy was evaluated; sequences with varying yaw angles were discarded.

3) The sequence size and the scale of the dolphin displacement were determined from the length of the dolphin.

Translated from Zhurnal Prikladnoi Mekhaniki i Tekhnicheskoi Fiziki, No. 2, pp. 160-164, March-April, 1971. Original article submitted April 14, 1970.

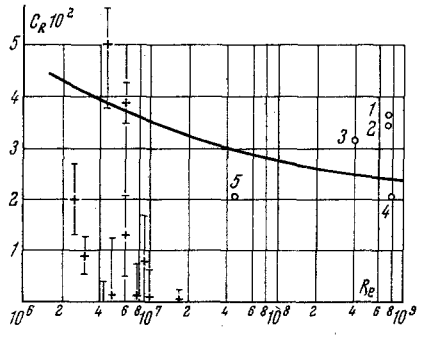

Fig. 1

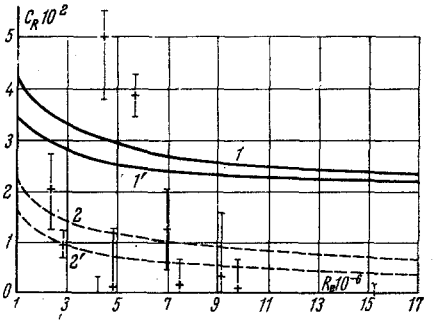

Fig. 2

4) The displacement scale of the sphere was determined.

5) The dolphin and sphere displacements over 5-7 frames were determined as a function of the dolphin velocity; the displacement was determined repeatedly (30-40 times) for each sequence, and the average displacement over these 5-7 frames, the rms error, and the simple error were calculated.

6) The dolphin velocity U_1 was calculated from

$$U_1 = U_0 \frac{\Delta b}{\Delta h},$$

where U_0 is the sphere velocity, Δb is the dolphin displacement, and Δh is the sphere displacement during the same time interval. The errors in the determination of the dolphin velocity were calculated.

7) The acceleration was determined by a time differentiation of the velocity, and the calculation error was determined. A numerical differentiation carried out for n points for each sequence yielded the average acceleration, the rms error, and the simple error. The latter values were compared to those found above; this comparison served as a check on the calculation error.

From the equation displayed above we calculated the drag; the dolphin dimensions were determined by direct measurement.

A clear advantage of this procedure for measuring the drag is that the dolphins are not subjected to any external agents during the experiments, and the flow pattern is not distorted by any type of pickup or attachment. On the other hand, an extremely important disadvantage of this procedure is the extensive data processing required. We therefore selected for careful study the most interesting sequences, i.e., those in which the dolphin moved rapidly, at a high Reynolds number.

2. Experimental Results

Figures 1 and 2 show the measured dolphin drag; the coordinates are the modified drag coefficient C_R and the Reynolds number Re:

$$C_R = \frac{2.10 v^{1/3}}{U_1^2} a, \qquad \mathrm{Re} = \frac{U_1 L}{\nu},$$

where v is the volume of the dolphin, L is its length, and ν is the kinematic viscosity of water.

These figures show both new results, for the dolphins Basya and Neptun, and experimental results from [1] for the dolphin Smelaya. Each cross represents the average value for n points; the error bars give the standard deviation from the average value. The values of n, the number of experimental points, for each sequence are as follows:

Sequence No.	9—9	9—17	9—19	9—20	9—24
$n =$	28	18	39	50	9
9—29	10—3	15—6	18—7	18—12	18—12.
6	26	46	34	72	65

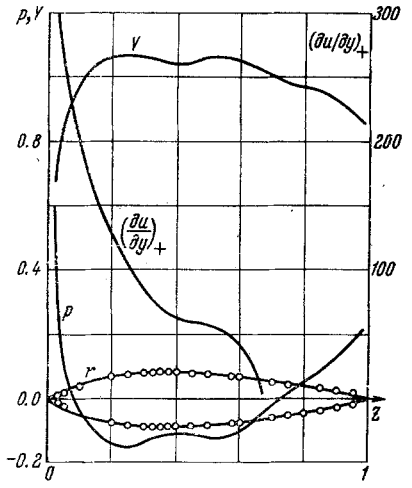

Fig. 3

For comparison, Fig. 1 shows experimental data for U. S. submarines and a full-scale torpedo [2]:

1. The submarine Nautilus (1), which has a classically shaped hull (L = 97.30 m, U = 23 knots, L/d = 11.4).

2. Submarines whose outer hulls are well-streamlined solids of revolution:

a) Skipjack (4) (L = 76.8 m, U = 30 knots, L/d = 7.8).
b) Tullibee (3) (L = 79.5 m, U = 15 knots, L/d = 8.9).
c) Thresher (2) (L = 85.0 m, U = 25 knots, L/d = 10).

3. The U. S. Navy torpedo MK-28 (5) (L = 6.25 m, U = 23 knots).

A calculated curve of the hydrodynamic drag for a model of the Skipjack is also shown. This calculation was carried out by the standard procedure [3] without an account of roughness for the case of turbulent flow. Comparison of these results with the experimental results for the dolphin show that in nine cases out of 11 the dolphin drag is several times lower (by a factor of 2-10) than that of the best submarine model.

The dolphin is therefore extremely efficient hydrodynamically. Figure 2 shows the drag of a solid equivalent to the dolphin under various flow conditions. The top curve corresponds to completely turbulent flow around the dolphin. This calculation was carried out by the procedure of [3] without an account of roughness. It was assumed for the calculation that there was laminar flow around the fins. A zero angle of attack was assumed for the fins.

Comparing these results with those calculated for the Skipjack model, we see that the dolphin shape is apparently nearly optimum in this case, since even in the case of turbulent flow the calculated drag coefficients of the dolphin model are approximately 1.5 below those for the Skipjack at equal Reynolds numbers.

Having taken note of this important result that the dolphin shape is nearly optimum, we must also note that Fig. 2 shows the dolphin drag to be much less than that of an equivalent solid model. The presence of the initial laminar-flow region reduces the calculated drag, but this decrease is slight [1] for Reynolds numbers greater than 6×10^6 for $Re_* = 2 \times 10^6$. In these experiments we found results for Reynolds numbers slightly greater than 1.5×10^7.

Accordingly, the conclusion reached in [1] that the motion of the dolphin is a unique hydrodynamic phenomenon has been confirmed in new experiments which are very reliable, for several reasons: First, the error is smaller (by a factor of about two); second, the experiments were carried out for higher Reynolds numbers; and third, we now have experimental proof for three Tursiops ponticus individuals. The existence of this unique hydrodynamic phenomenon also follows from the arisal of Gray's paradox. In two cases out of 11, however, a drag greater than the calculated drag for the equivalent dolphin model was found in turbulent flow. Although an explanation can be found in the presence of a rudder angle of the tailfin in sequence 9-24, which would increase the drag, there is no plausible explanation for sequence 15-6. In this sequence the dolphin moves horizontally, and the rudder angle of its tailfin is nearly zero. Presumably the explanation for the low dolphin drag is to be found in some controllable mechanism.

Let us analyze some hypotheses which have been advanced to explain this phenomenon. We turn first to the model of the dolphin. Direct measurements show that the cross-sectional area of the dolphin is elliptical; for a large part of its length the ellipticity is slight, or the cross section is nearly circular. We calculated the equivalent solid of revolution on the basis of equal areas at each cross section, completing the shape with a smooth curve. The solid of revolution constructed in this manner corresponds approximately to model 25, for which computer calculations were carried out of the potential-flow characteristics and the laminar boundary layer at the Computer Center, Siberian Branch, Academy of Sciences of the USSR [4].

Figure 3 shows the relative potential-flow velocity V for this model, the relative hydrodynamic overpressure P, and the relative laminar tangential stress at the wall $(\partial u/\partial y)_+$. Kramer has suggested [5] that the good performance of dolphins can be attributed to the preservation of a laminar boundary layer through the damping of pulsations in this layer by the elasticity of the surface. This method does not assume a change in the potential flow pattern.

This calculation should thus be valid for laminar flow about an elastic boundary. At $z = 0.696$, however, the laminar boundary layer is disrupted, and a large additional drag appears because the pressure is not reestablished at the tail. The drag coefficient calculated for this case is shown by the lower solid curve in Fig. 2. We see that when the boundary layer is disrupted, laminar flow does not lead to a significant reduction of the total drag below that corresponding to completely turbulent flow. If it were possible to prevent the disruption of the boundary layer by some method without increasing the energy expenditure, the situation would change radically. The lower broken curve in Fig. 2 shows the drag calculated for the dolphin model in the case of laminar flow, carried out under the assumption of a vanishing separation drag. In this case there is no significant difference between the calculated and experimental data, except for sequences 10-3 and 18-7, for which the results lie below the calculated curve. It should be noted, however, that the frictional drag in motion at a constant negative acceleration (i.e., for the conditions corresponding to the experiment described) is slightly less than the drag in steady-state flow.

The upper broken curve in Fig. 2 shows the drag calculated for the dolphin model for the case of mixed flow: laminar from the nose to $z = 0.687$, i.e., essentially up to the separation point; and turbulent from $z = 0.687$ to $z = 1$. This calculation was carried out by the Trukenbrodt method [6]; the laminar-friction characteristics for the model were taken from the computer calculation of [4], and the two solutions were joined at the transition from laminar to turbulent flow on the basis of the momentum-loss thickness. We see that in this case there is a discrepancy between calculation and experiment for five sequences, so we must apparently reject this explanation. Accordingly, of the schemes considered, laminar undetached flow corresponds best to experiment in terms of drag. Two problems of fundamental importance arise:

1. How can a critical Reynolds number $Re_* > 10^7$ be achieved for a solid of revolution in a region with a positive potential gradient in flow with a nonvanishing turbulence level?

2. How can the separation of the laminar boundary layer at the tail be prevented?

Note. After this paper was completed, the authors learned of a report by professor Wu [7] of the California Institute of Technology in which he presented experimental data on drag values found by Lang for the dolphin Tursiops gilli (native to the Pacific Ocean) and reached the conclusion that laminar flow apparently occurs aound this dolphin.

Accordingly, analogous results have been obtained in two independent studies for two very similar types of dolphin.

LITERATURE CITED

1. B. N. Semenov, "Existance of a unique hydrodynamic phenomenon of the dolphin," in: Bionics [in Russian], No. 3, Naukova Dumka, Kiev (1969).
2. V. M. Bukalov and A. A. Narusbaev, Design of Atomic Submarines [in Russian], Sudostroenie, Leningrad (1964).
3. Yu. I. Voitkunskii, R. Ya. Pershishch, and I. A. Titov, Handbook on the Theory of Ships [in Russian], Sudpromgiz, Leningrad (1960).
4. T. E. Alekseeva, V. P. Gromov, A. F. Dmitrieva, B. P. Kolobov, B. G. Kuznetsov, B. N. Semenov, and N. N. Yanenko, Calculation of the Characteristics of Laminar Boundary Layers on Solids of Revolution [in Russian], Nauka, Novosibirsk (1968).
5. M. O. Kramer, "The dolphin's secret," J. Amer. Soc. Naval Engrs, 73, No. 1 (1961).
6. H. Schlichting, Boundary-Layer Theory, McGraw-Hill (1968).
7. T. Yau-tsu Wu, "Fluid mechanics of swimming propulsion," Paper Presented to the 7th Symposium on Naval Hydrodynamics, Rome, August 25-30, 1968.